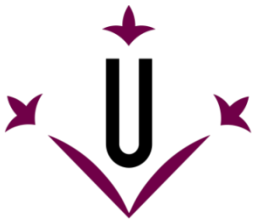

*Graphical Abstract

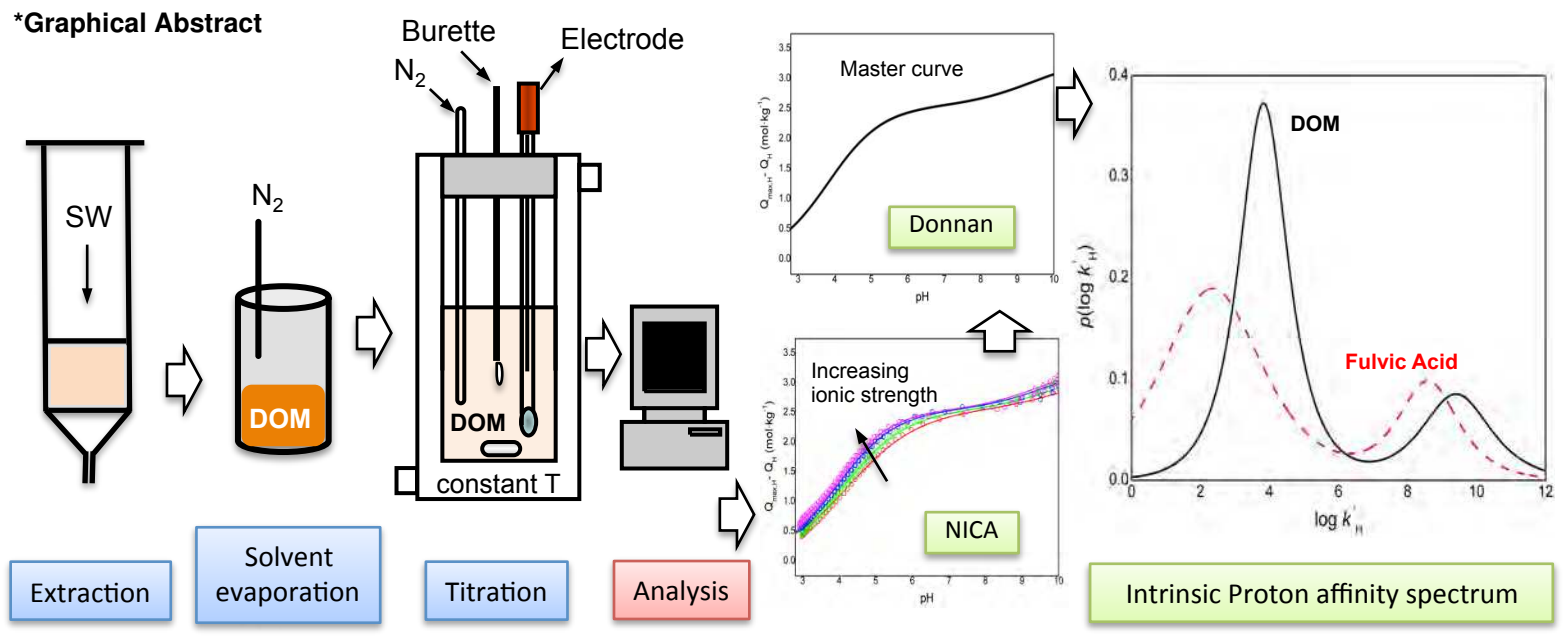

***Highlights (for review : 3 to 5 bullet points (maximum 85 characters including spaces per bullet point)**

- Marine dissolved organic matter affects trace metals biogeochemistry and carbon cycle
- Research the acid-base properties of DOM is key to unravel its role in marine systems
- Potentiometric titrations allow us studying the proton binding to marine DOM
- Marine DOM is compared with fulvic acids in terms of NICA-Donnan parameters
- Variation in proton binding parameters has potential effects for Fe binding by DOM

Acid-base properties of dissolved organic matter extracted from the marine environment.

Pablo Lodeiro[a*], Carlos Rey-Castro[b], Calin David[b], Eric P. Achterberg[a], Jaume Puy[b] and Martha Gledhill[a]

[a]GEOMAR Helmholtz Centre for Ocean Research Kiel, Wischhofstraße 1-3, 24148 Kiel, Germany

[b]Departament de Química, Universitat de Lleida and AGROTECNIO, Rovira Roure 191, 25198, Lleida, Spain

*Corresponding Author: plodeiro@geomar.de

Keywords: marine DOM; NICA-Donnan; proton binding; intrinsic pK_a; trace metal availability

https://doi.org/10.1016/j.scitotenv.2020.138437

Abstract

Marine dissolved organic matter (DOM) plays a key role in the current and future global carbon cycle, which supports life on Earth. Trace metals such as iron, an essential micronutrient, compete with protons and major ions for the binding to DOM. These competitive effects and the DOM binding capacity are related to the DOM acid-base properties, which also influence DOM transport and reactivity in marine waters. Here we present the results of a complete set of acid-base titration experiments of a pre-concentrated marine DOM sample in the range $0.01 \leq I \leq 0.7$ M and $3 \leq pH \leq 10$. We characterize the obtained proton binding curves using a combination of the non-ideal competitive adsorption (NICA) isotherm and Donnan electrostatic model. Within the main chemical groups of marine DOM, the carboxylic distribution was accurately characterized from the obtained data ($Q_{\max H,1}$=2.52 mol·kg^{-1}, $\log \overline{k}_{H,1} = 3.26$, $m_1 = 0.69$ and $b = 0.70$). This carboxylic mode was found to be less acidic and more homogeneous than a generic fulvic acid, but the differences are consistent with the reported variability of fulvic acids of freshwater and terrestrial origin. We find that changes in temperature (down to 5.5ºC), and the presence of calcium or magnesium (at 0.01 M) resulted in no significant modification of the proton ion binding curves obtained at 25ºC and 0.7 or 0.1 M ionic strength, respectively. We demonstrate the relevance of proton binding parameters for the modelling of the system iron/marine DOM throughout a wide range of salinity and acidity conditions in the context of different future ocean scenarios.

1. Introduction

Dissolved organic matter (DOM) forms one of the largest bioactive carbon reservoirs on Earth and plays a key role in the global carbon cycle (Carvalhais et al., 2014; Hansell, 2013). Marine DOM supports heterotrophic activity and forms complexes with (micronutrient) trace metals, affecting their availability and thus primary production and toxicity. Therefore, marine DOM has major relevance for biogeochemical and climate systems.

Marine DOM is formed of structurally complex and poorly defined compounds (Zark and Dittmar, 2018). The analysis of chemical groups at a molecular level only accounts for <10% of the DOM pool to date (Repeta, 2015). Carbohydrates, polysaccharides and proteins have been identified as major chemical components of marine labile and semi-labile DOM within the upper water column (Repeta, 2015). Whilst marine DOM is inherently heterogeneous, carboxylic acids are nevertheless one of the main chemical functionalities in its structure followed in a smaller proportion by phenolic compounds (Hawkes et al., 2019; Hertkorn et al., 2006). Thus, marine DOM possesses fundamental acid-base properties, although investigation of these properties has received little attention to date (Cai et al., 1998; Huizenga and Kester, 1979; Powers et al., 2019; Ulfsbo et al., 2015).

The acid-base behaviour of marine DOM can influence its interactions with particles, including marine microbes, and the description of organic alkalinity of seawater, affecting CO_2 system calculations and thus biogeochemical models of the carbon cycle (Kuliński et al., 2014). Moreover, the binding of trace metals to marine DOM is controlled by the acid-base properties of DOM and the characteristics of the various chemical species of the metals in seawater, which both depend on pH, ionic strength, temperature, and solution composition (Tipping, 2002). All these factors act in

76 combination impacting biological activity, which is also linked to marine DOM
77 cycling. For example, dissolved iron is bound in more than 99% to organic ligands.
78 Since iron limits productivity in as much as 30% of the surface ocean, the overall
79 impact of organic complexation of iron is to increase the dissolved and thus
80 bioavailable iron pool (Gledhill and Buck, 2012). Both iron hydrolysis and iron
81 binding to DOM are strongly influenced by pH, yet a thorough parameterisation of
82 these interactions is currently lacking (Avendaño et al., 2016; Gledhill and van den
83 Berg, 1994; Turner et al., 2016).
84 Potentiometric titrations using glass/selective electrodes are routinely applied for the
85 physicochemical analysis of *e.g*. biomass (Lodeiro et al., 2019) and fulvic and humic
86 substances of terrestrial or freshwater origin (David et al., 2010; Koopal et al., 2005).
87 In coastal waters like the Baltic Sea, a significant part of the DOM pool is of
88 terrestrial origin and supplied by rivers (Deutsch et al., 2012; Hoikkala et al., 2015;
89 Seidel et al., 2017), although overall a very small fraction of terrestrial DOM (<0.03
90 %) is exported to the ocean (Cai et al., 1998; Carlson and Hansell, 2015; Dittmar and
91 Stubbins, 2014).
92 The direct physicochemical analysis of marine DOM has proved difficult due to its
93 low concentration, especially in open-ocean environments (< 1 mg/L) (Martín
94 Hernández-Ayon et al., 2007; Yang et al., 2015). Improvements in pre-concentration
95 and isolation techniques such as solid-phase extraction (SPE) have now provided us
96 with powerful tools for marine DOM chemical characterization (Repeta, 2015). Solid-
97 phase extraction mostly isolates hydrophobic fractions of marine DOM and some
98 polar compounds based on well established protocols (Dittmar et al., 2008), with
99 extraction efficiencies >30% for DOC recovery. Pre-concentration techniques
100 selectively restrict the fraction of DOM that is being analysed, which limits our

understanding of the full DOM composition. Nevertheless, a careful selection of extraction conditions (flow rate, loading masses and pH) can provide us with DOM extracts that are highly representative for the original seawater sample (Li et al., 2016; Li et al., 2017).

Like marine DOM, terrestrial and aquatic humic-like substances are composed of a large range of different complex molecules. Despite this complexity, generic binding parameters have been obtained, included in speciation software, and used for modelling purposes (Milne et al., 2001; Rey-Castro et al., 2009). We postulate that a similar approach can be implemented for marine DOM in order to allow for the examination of competitive interactions between cations and protons in seawater, and thus a fuller understanding of the impact of ocean acidification on trace metal biogeochemistry in the ocean.

We present here a complete physicochemical study of the acid-base properties of marine DOM isolated from surface Baltic seawater using solid-phase extraction. We applied a simple potentiometric technique for identification of major classes of active chemical groups and measurement of proton binding properties of marine DOM. We used a combination of the non-ideal competitive adsorption (NICA) isotherm that accounts for the specific -chemical- ion binding, and the Donnan model for electrostatic effects (Kinniburgh et al., 1999; Koopal et al., 1994).

Furthermore, we investigated the potential competitive binding effects with two major divalent cations in seawater, *i.e.*: magnesium and calcium, and the influence of temperature on proton binding (Milne et al., 2001). Finally, we address the potential impact of pH and salinity changes on the protonation state of the main chemical groups present in marine DOM with relevance for the binding of iron, and other trace metals.

2. Material and methods

2.1 Seawater collection

Seawater samples were collected in June and July 2019 in a Baltic fjord located in northwest Germany (54.33ºN 10.15ºE). Surface water (ca. 0.2 m depth) was collected using 20 L acid cleaned high density polyethylene (HDPE) and fluorinated HDPE carboys. A total of approximately 200 litres of water were filtered through 0.45/0.2 μm cellulose acetate membrane filters (Sartobran 300, Sartorius) and subsequently acidified with concentrated HCl (Romil UHP grade) to a final concentration of 0.1 % (v/v). In order to check for potential organic contamination from the clean carboys used for sampling, three of them were filled with high-purity water with a resistivity of 18.2 MΩ cm^{-1}, and stored overnight. Dissolved organic carbon (DOC) was subsequently measured in triplicate for each of the three carboys (carboy carbon blank).

2.2 Dissolved organic matter extraction

Dissolved organic matter was extracted from the filtered/acidified seawater using Mega Bond-Elut PPL (5 g, 60 mL) solid-phase extraction cartridges (Agilent). The 10 PPL cartridges used were soaked for 12 h with 50 mL of methanol (Fisher Scientific LC-MS grade), and then washed passing 15 mL of HCl 0.1% (v/v) through each cartridge before use. After passing the seawater through, the PPL cartridges were washed with 15 mL of high-purity water, and then soaked during 10 min with (2 x) 10 mL of acetonitrile to finally extract the DOM. The acetonitrile-DOM solution (20 mL from each cartridge) was collected in a Teflon™ pot (250 mL) and dried under a stream of ultrapure N_2 gas for c.a. 24 hours. The extraction efficiencies were determined as DOC content of the original water sample versus DOC in the extracted

151 seawater after passing 9-12 L through each PPL cartridge. Blanks were obtained in
152 triplicate by extracting high-purity water following the same procedure as for the
153 seawater samples, and determining the DOC concentration in the extracts.

154 **2.3 Dissolved organic matter stock solution**

155 The extracted solid sample (0.74 g) was dissolved in 100 mL of NaOH 0.02 M, and
156 preserved in the dark at 4ºC. This DOM stock solution was diluted and used for the
157 titration experiments.

158 **2.4 Seawater analysis**

159 A detailed description of the seawater analysis for nutrients (phosphate, silicic acid,
160 nitrate and nitrite), dissolved organic/inorganic carbon, pH, total alkalinity,
161 temperature and salinity, can be found in the Supplementary Material.

162 **2.5 Potentiometric titrations**

163 An automatic titration system controlled with a homemade Matlab script was used for
164 the titration experiments. The system consisted of a burette (Metrohm, Dosimat 765)
165 with a capacity of 1 mL, and a benchtop pH meter (Thermo Orion, 720Aplus) both
166 connected to a computer. The electromotive force between a glass electrode
167 (Metrohm 6.0133.100) and a reference electrode (Metrohm 6.0726.100), with a NaCl
168 jacket at a concentration that matches the ionic strength of the titrated solution, was
169 monitored and recorded using a drift criterion of <0.05 mV/min, with a maximum
170 stabilization time of 120 min. The electrodes were calibrated before each DOM
171 titration in terms of hydrogen ion concentration (Brandariz et al., 2004) using the
172 same ionic strength and potential drift criterion as for the corresponding experiment.
173 Duplicate titrations were performed under water-saturated nitrogen bubbling in a
174 sealed thermostated vessel containing 20 mL of a diluted DOM solution. This solution
175 was made of 10 mL of DOM stock plus different amount of 2 M NaCl (Merck, p.a.)

176 to set the ionic strength and standardised 0.1 M HCl (Honeywell, Fluka^{TM}) to obtain a
177 solution pH 3.0, and diluted with high-purity water. The DOM concentration in all
178 solutions titrated was 1.48 ± 0.07 g DOM·L^{-1} (436 mg C·L^{-1}). The ionic strength of
179 the titrated solutions was fixed to values of 0.01, 0.02, 0.1 and 0.7 M using NaCl as
180 inert supporting electrolyte. The temperature was kept at 25ºC using a controlled
181 temperature bath circulator (Thermo Scientific, A10). For the highest ionic strength
182 (0.7 M) experiments at 5.5 and 15ºC were also performed. Standardised 0.1 M NaOH
183 (Honeywell, Fluka^{TM}) was added using the burette at 0.025 mL intervals to perform
184 the titration experiments. A typical DOM titration experiment took about 6-8 h.
185

186 **3. Theory and calculations**

187 **3.1 The NICA-Donnan model**

188 The proton titration data was described by the combination of a bi-modal NICA
189 isotherm and the Donnan electrostatic model (Kinniburgh et al., 1996; Kinniburgh et
190 al., 1999; Koopal et al., 1994; Rey-Castro et al., 2009).
191 In the absence of metal cations able to compete with protons for the specific binding
192 to the functional groups of DOM (mono-component system), the bi-modal NICA
193 isotherm for proton binding is formally identical to the weighted sum of two
194 Langmuir-Freundlich isotherms (Milne et al., 2001):

195 $$Q_H = Q_{\mathrm{maxH,1}} \frac{\left(\overline{k}_{\mathrm{H,1}} c_{\mathrm{H,D}}\right)^{m_1}}{1+\left(\overline{k}_{\mathrm{H,1}} c_{\mathrm{H,D}}\right)^{m_1}} + Q_{\mathrm{maxH,2}} \frac{\left(\overline{k}_{\mathrm{H,2}} c_{\mathrm{H,D}}\right)^{m_2}}{1+\left(\overline{k}_{\mathrm{H,2}} c_{\mathrm{H,D}}\right)^{m_2}} \quad (1)$$

196 where Q_{H} stands for the amount of bound protons (mol·kg^{-1}), $Q_{\mathrm{maxH,j}}$ is the total
197 amount of available proton binding sites within each distribution, $\log \overline{k}_{\mathrm{H},j}$ is the
198 median value of the j^{th} affinity distribution for protons, $c_{\mathrm{H,D}}$ is the proton

199 concentration at the Donnan phase, and m_j ($0 < m_j \leq 1$) is a parameter related to the
200 width of the affinity distribution function (a measure of the apparent binding
201 heterogeneity). The limiting value of $m_j = 1$ corresponds to a perfectly homogeneous
202 set of sites. The subindexes $j = 1$ and 2 represent the most and less acidic modes in the
203 affinity distribution of sites, usually associated to carboxylic and phenolic functional
204 groups, respectively.
205 In the presence of bound Ca or Mg (major cations in seawater) or trace metal ions, the
206 system is multi-component and the corresponding competitive NICA expressions are
207 detailed in the Supplementary Material.
208 The electrostatic contribution to the effective ion binding is accounted for by the
209 Donnan model, which assumes that DOM behaves as an electroneutral, permeable gel
210 phase with a homogeneous distribution of fixed charges (resulting from the
211 dissociation of proton binding functional groups) (Benedetti et al., 1996a; Kinniburgh
212 et al., 1996). The value of the gel phase volume in the Donnan model, V_D, is critical
213 for the ability of the model to accurately reproduce the influence of ionic strength on
214 the shapes of the titration curves. Despite its empirical nature, it is expected to
215 reproduce the influence of the environmental variables such as pH or charge on the
216 hydrodynamic size of the macromolecule. In the absence of experimental estimates,
217 V_D has been used as a variable to fit the obtained charge curves. The usual fit
218 convergence criterion is the merging of these curves, obtained at different ionic
219 strengths, when they are plotted against the local pH value in the Donnan phase, pH_D,
220 defined as $\log c_{H,D}$ (termed the '*master curve*') (Benedetti et al., 1996b).
221 Three different models of V_D are compared in this work: 1) standard (or classical) V_D
222 model; 2) V_D consistent with Poisson-Boltzmann (PB-V_D); 3) '*Ad hoc*' V_D values.

The equations and descriptions of the Donnan sub-models used in this work are detailed in the Supplementary Material.

3.2 Strategy for the derivation of NICA-Donnan model parameters

The experimental datasets (titrant volume, pH) obtained at each ionic strength were converted into (pH, charge) curves using a charge balance relationship, as detailed in the Supplementary Material (eq. S7). Note that pH was measured on the hydrogen ion concentration scale, as described in section 2.5. The optimization of the NICA-Donnan parameters was carried out by non-linear regression using MATLAB (2019) to minimize the root-mean square error (RMSE, in mol·kg^{-1}) in the DOM charge:

$$\mathrm{RMSE} = \left[\frac{\sum_{i=1}^{N} \left(q_i \quad \hat{q}_i \right)^2}{N \quad l} \right]^{1/2} \tag{2}$$

where $\hat{q}_i$ is the fitted value, N the number of data points and l the number of model parameters.

In principle, all 6 intrinsic binding constants for proton can be fitted simultaneously together with the V_D model variable. However, the relatively high degree of covariance among parameters often requires a suitable strategy to constrain the convergence within realistic values. In fact, the characterization of the phenolic distribution from our experimental data proved to be rather uncertain due to poor reproducibility and limited pH range. For this reason, the binding parameters of the second mode were constrained as follows:

- Standard V_D model: the values of $\overline{k}_{\mathrm{H},2}$, m_2, and the ratio $Q_{\max H,1} / Q_{\max H,2}$ were kept fixed to the corresponding values of the generic NICA parameters for FA (Milne et

al., 2001), while the remaining four parameters ($Q_{\max H,1}$, $\overline{k}_{H,1}$, m_1 and b) were optimized.

- PB-V_D model: the ratio $Q_{\max H,1}/Q_{\max H,2}$ was constrained to the generic value for FA, and values of $\overline{k}_{H,2}$ and m_2 were kept fixed to the apparent (conditional) values estimated at I = 0.7 M from the generic FA parameters. In this way, the remaining degrees of freedom in the fits were $Q_{\max H,1}$, $\overline{k}_{H,1}$, m_1 and a.

- '*ad hoc*' V_D model: the same as for the PB-V_D model, but in this case also the intrinsic values of $Q_{\max H,1}$, $\overline{k}_{H,1}$ and m_1 were directly fitted from the conditional curve at I = 0.7 M (which is assumed equivalent to the master curve) and, thus, values of V_D at I = 0.01, 0.02 and 0.1 M were optimized to fit the corresponding titration curves.

4. Results

4.1 Marine DOM extracted sample

The marine DOM sample used in the titration experiments was preconcentrated from a surface seawater (Kiel Baltic fjord) with salinity 16 (I = 0.32 M), pH 8.36 ± 0.06 and temperature of 16.6 ºC. Values of 2087 ± 9 and 1887 ± 10 μmol·kg^{-1} were obtained for total alkalinity and dissolved inorganic carbon, respectively. The concentrations of macronutrients were 15.79 ± 0.29 (silicic acid), 0.76 ± 0.23 (phosphate) and 0.11 ± 0.01 (nitrate + nitrite) μmol·kg^{-1}. We calculated an average extraction efficiency of 39 ± 6 % for DOC recovery. The measured DOC concentration was 296 ± 5 μmol·kg^{-1} in the seawater sample, and 182 ± 10 mmol C·L^{-1} in the prepared DOM stock solution (which corresponded to *ca*. 7.4 g DOM·L^{-1}). Carboy carbon blanks showed DOC values (3.16 ± 5.99 μmol/L) of the same order of

magnitude of the blanks (acidified high-purity water) run in DOC analysis. The blanks for the PPL extraction procedure also yielded negligible DOC values (3.42 μmol C) with a contribution of C to the DOM stock solution below 0.1%. Thus, we observed a negligible carbon contribution from the SPE cartridges or filters that we used in our study.

4.2 Acid-base properties of marine DOM

Figure 1 shows the comparison between experimental data and model fits using the optimized parameter values listed in Table 1. Figure 2 shows the density of probability of proton binding affinities (i.e., the affinity spectra) of marine DOM sites for two different reference states: a) intrinsic conditions (*i.e.*, chemical binding affinities); and b) effective conditions (chemical plus electrostatic binding) at the sampling site, *i.e.*: I = 0.32 M. The corresponding spectra calculated with the NICA-Donnan parameters of a generic fulvic acid were included for comparison in both cases. The intrinsic affinity spectra in panel (a) reflect the binding characteristics of the master curves obtained with each of the three Donnan models studied. Panel (b) also shows the density of protonated sites for marine DOM at pH 8.36. The spectra were calculated as described in (Rey-Castro et al., 2009) (see Supplementary Material).

4.3 Marine DOM Donnan volumes and radii

Figure 3 shows the values of V_D obtained with the different Donnan models compared in this work and those obtained from the generic value of b for fulvic acids. **Table 2** includes a summary of values (radii and average distance between charges) derived for marine DOM on the basis of the fitted values of V_D.

4.4 Effect of temperature and presence of major ions on proton binding

Table S1 shows the mean affinity of the 1st (carboxylic) distribution obtained from titrations at I = 0.7 M in the range between 5.5 and 25ºC. The experimental data and NICA-Donnan predictions of the titrations carried out in 0.01 M Ca^{2+}/Mg^{+2} (at I = 0.1 M) are shown in **Figure S1**.

4.5 Relevance to modelling of trace metal binding by marine DOM

Figure 4 shows theoretical NICA-Donnan predictions of iron binding by marine DOM using two different combinations of proton binding parameters, for a range of salinity (S) and pH conditions representative of surface waters in the Baltic Sea, and assuming inorganic dissolved iron controlled by the solubility of $Fe(OH)_{3(s)}$. These calculations are only intended to illustrate the importance of an exhaustive characterization of acid-base and electrostatic features of marine DOM as a first approximation in the development of predictive models for the effects of climate change scenarios on the availability of trace metals in the ocean.

5. Discussion

5.1 Seawater analysis

The sampled surface brackish water presents typical characteristics of sea areas influenced by both terrestrial freshwater inputs and seawater inputs from the North Sea. The high pH value obtained (8.36) is consistent with surface waters at the end of a phytoplankton bloom, which is confirmed by relatively low nutrient concentrations. Since the water was post-bloom, it is likely there was intense production of autochthonous organic matter, which contributed to high DOC values (296 $\mu mol \cdot kg^{-1}$). Moreover, we measured relatively low alkalinity and dissolved inorganic carbon concentrations of ca. 2000 $\mu mol \cdot kg^{-1}$, which is a typical value for this kind of large estuarine systems (Kuliński et al., 2014).

316 **5.2 Acid-base properties of marine DOM**

317 The experimental acid-base titration curves of the extracted marine DOM at 25ºC
318 show the typical shape of a bi-modal Langmuir-Freundlich isotherm. These curves
319 were successfully fitted with the mono-component NICA-Donnan model for proton
320 ions within the range $0.01 \leq I \leq 0.7$ M and $3 \leq pH \leq 10$ (Figure 1). The values of
321 RMSE (Table 1) are comparable to those obtained from fits of individual datasets of
322 terrestrial and freshwater fulvic acid samples, and are certainly lower than values
323 (RMSE = 0.123) obtained with the collective dataset used to derive the generic NICA
324 parameters for FA (Milne et al., 2001). Therefore, and from a purely empirical point
325 of view, the combination of NICA and the standard Donnan model proved to be an
326 accurate descriptor of the proton binding behavior of marine DOM.
327 We were able to accurately characterize and fit the 1st group of binding sites (the low
328 affinity distribution) from the experimental titration data (Table 1). However, for the
329 2nd group (the high affinity distribution), a direct (unconstrained) fitting yielded
330 excessively wide confidence intervals for $\overline{k}_{H,2}$ and m_2 values. This was a result of *i*)
331 little overlap between both distributions, as shown in Figure 1, and *ii*) relatively poor
332 reproducibility of experimental data above pH 9. We therefore decided to fix $\overline{k}_{H,2}$ and
333 m_2, as well as the $Q_{\max H,2}/Q_{\max H,1}$ ratio, to the generic values of the phenolic groups
334 of FA (Milne et al., 2001), as explained in section 3.2. This restriction in the degrees
335 of freedom did not increase the value of the RMSE substantially, as compared with
336 the optimization of the full set of NICA parameters (data not shown). This suggests
337 that the generic phenolic parameters of FA might be close to the actual intrinsic
338 values of the 2nd distribution of marine DOM sites. In any case, future work should be
339 carried out within an extended pH interval and a reduced tolerance in the mV/min

shift criterion in order to achieve a more robust assessment of the features of the high affinity binding sites.

We observed some differences between our marine DOM and the typical behavior of fulvic acids of terrestrial origin:

1) Number of titratable groups: Our marine DOM has a relatively small amount of groups (2.52 $mol \cdot kg^{-1}$) as compared with average (generic) values reported for FA (*ca*. 6 $mol \cdot kg^{-1}$). Here, we would like to highlight the potential bias introduced by the technique used to preconcentrate our marine DOM sample. Solid-phase extraction of marine DOM using PPL columns tends to selectively retain hydrophobic compounds. Moreover, the extraction yield is usually far from being complete, with a 39 % recovery based on DOC values in our case. This selective and incomplete DOM extraction procedure could therefore limit the number and type of chemical compounds analyzed in the titration experiments. Nevertheless, we selected the experimental conditions based on previous studies that suggest that marine DOM extracted at pH 2 using PPL cartridges is representative of bulk marine DOM (Green et al., 2014; Li et al., 2016; Li et al., 2017). To confirm this, further validation and improvement of the extraction methods with respect to retention of polar components will be an objective for future research. In any case, the methodology of this work may be extended to the individual characterization of separate DOM fractions collected through a multi-stage sequential extraction scheme (using e.g. adsorption resins of different hydrophobicity). The collective behaviour of the whole DOM in the original seawater sample could, then, be described by the weighted average (relative to the respective number of binding sites) of the spectra corresponding to each individual fraction of DOM (Christl and Kretzschmar, 2001; Pernet-Coudrier et al., 2011).

365 2) Intrinsic (chemical) proton affinity: The fitted NICA parameters indicate that the
366 low affinity distribution of marine DOM is slightly less acidic and significantly more
367 homogeneous than an average FA, which presents generic values of $\log \overline{k}_{H,1} = 2.34$ and
368 $m_1 = 0.38$ (recall that $m = 1$ corresponds to a perfectly homogeneous distribution).
369 The differences in proton binding behaviour between marine DOM and the generic
370 FA can be visually identified in the intrinsic affinity spectra of Figure 2a. Still, the
371 variability observed in literature in the NICA parameters obtained from individual fits
372 to specific FA samples is substantial. For instance, Milne et al. (Milne et al., 2001)
373 report the following min-max ranges: $2.64 < Q_{\max H,1} < 8.76$ mol·kg^{-1}; $2.00 < \log \overline{k}_{H,1} <$
374 3.81; and $0.27 < m_1 < 0.65$ in an ensemble of 25 datasets. In conclusion, the
375 characteristics of the most acidic mode of the marine DOM fraction are notably
376 different from the carboxylic mode of an average (generic) FA, but the deviations are
377 almost within the observed natural variability between samples.
378 3) Effective (conditional) proton affinity: The generic NICA-Donnan set of
379 parameters for FA lead to effective binding spectra that are clearly different from
380 those of marine DOM as displayed in Figure 2b for the particular case of $I = 0.32$ M.
381 At these conditions, the effective affinity spectrum of marine DOM shows a first peak
382 (with a maximum at $\log \overline{k}_{H,1} = 3.8$) that is noticeably narrower (*i.e.*, less
383 heterogeneous) and slightly shifted to larger affinities (0.3 log units) as compared
384 with the generic FA. For the standard V_D model, the fitted value of b (0.70) is above
385 the generic FA value (0.57), indicating that the values of V_D in the marine DOM
386 fraction are somewhat larger (and more sensitive to variations in ionic strength) than
387 in a generic FA. Yet the high variability observed ($0.29 < b < 0.94$) in fits of
388 individual fulvic datasets (Milne et al., 2001) suggests, again, that the electrostatic

389 behaviour of marine DOM may not be inherently different from that of a terrestrial
390 FA. However, one controversial issue remains. As seen in Figure 1, the master curve
391 obtained with the standard Donnan model deviates significantly from the titration
392 curve at I = 0.7 M, suggesting that electrostatic effects are still relevant at this high
393 ionic strength, which does not seem plausible. This is the reason why an alternative fit
394 with the other two models was carried out as a comparison.
395 As regards the PB-V_D and '*ad hoc*' models, it can be noticed (see Table 1) that the
396 total amount of sites obtained from fitting is almost the same as in the standard model
397 (3.36 - 3.32 mol·kg^{-1}), but the intrinsic (chemical) values of the low affinity
398 distribution now display larger average and variance values (Figure 2a), *i.e.*: the 1st
399 group of sites are less acidic and more heterogeneous than in the standard model. It
400 must be noted that the differences among the three different Donnan models lie
401 mainly on how the free energy of proton binding is split into intrinsic (chemical) and
402 electrostatic contributions. Indeed, the effective (overall) binding affinity distributions
403 at a given ionic strength for marine DOM are almost indistinguishable from each
404 other.
405 When we compare our PPL-extracted DOM with the only study found on acid-base
406 properties of extracted marine DOM (Huizenga and Kester, 1979), we observed
407 certain similarities:
408 1) The number of titratable groups of the first mode of our DOM (8.56 mmol/g C) is
409 close to the lower range of the values, 8.96-13.82 mmol/g C, shown by Huizenga and
410 Kester (Huizenga and Kester, 1979) for DOM isolated by activated charcoal
411 adsorption from river, estuarine, coastal, and open ocean waters.
412 2) The log K values obtained by Huizenga and Kester (Huizenga and Kester, 1979) in
413 $NaClO_4$ 0.7 m for the eight samples of marine DOM studied lie between 3.33 and

414 3.75, which is in agreement with the value that we calculated for the first mode, 3.79
415 at 0.7 M NaCl.
416 These authors present results within the pH range 2-8, and therefore they were not
417 able to characterize the binding sites with affinity distribution associated to phenolic
418 functional groups.

419 **5.3 Marine DOM Donnan volumes and radii**

420 The values of V_D (Figure 3) show in all cases a decreasing trend with I, which is the
421 expected behaviour due to screening of intramolecular electrostatic repulsion. The
422 values obtained with the PB-V_D and '*ad hoc*' models are very similar and significantly
423 larger than those fitted with the standard model. Consequently, the former two models
424 yield master curves that lie close to the curve at the highest ionic strength, which is a
425 reasonable behavior. However, these relatively large values of V_D, may lose some of
426 the underlying theoretical significance. For instance, the PB-V_D sub-model leads to a
427 fitted value of a = 0.036 kg·mol$^{-1/2}$·L$^{-1/2}$ (Table 1) which corresponds to a solid-sphere
428 radius of 0.1 nm (assuming ρ = 1.4 kg·L^{-1}). This value is representative of a molecular
429 (rather than nanoscopic) scale. Additionally, the V_D values obtained with standard and
430 '*ad hoc*' models are translated here into estimated DOM radii on the basis of a
431 reference molecular weight value for marine DOM of 500 Da, in agreement with the
432 values reported in literature (Dittmar and Stubbins, 2014; Hawkes et al., 2019; Seidel
433 et al., 2017). In the standard model, the sizes obtained (Table 2) are just below the
434 characteristic Debye lengths (^{1}) at the corresponding ionic strengths up to 0.1 M,
435 and the average charge-charge distance becomes close to ^{1}already at 0.02 M,
436 whereas the '*ad hoc*' model predicts consistently larger dimensions. Thus, the size
437 and charge distribution of marine DOM (particularly at high ionic strength) might not
438 be fully consistent with the postulates of the Donnan model (Ohshima, 2006;

439 Ohshima, 2008). A more realistic description of the electrostatic effects (probably
440 through an oligoelectrolyte model) seems then to be required, although it lies out of
441 scope of this work. Nevertheless, the use of the NICA-Donnan model is still relevant,
442 as it allows us to compare the behavior of the isolated marine DOM fraction with the
443 generic descriptions of fulvic acids of terrestrial and freshwater origin, in terms of the
444 average and variance of the corresponding proton affinity distributions (Figure 2).

445 **5.4 Effect of temperature and presence of major ions on proton binding**

446 We observed no difference in the titration curves obtained at three different
447 temperatures beyond experimental uncertainty. Still, we could estimate an upper
448 bound for the absolute value of the average protonation enthalpy of the carboxylic
449 sites as 4 $kJ \cdot mol^{-1}$ (see Supplementary Material), which is consistent with previous
450 literature reports (Xu et al., 2018).

451 The effects of calcium and magnesium ions on the proton binding to marine DOM
452 were also investigated, with inconclusive results. Acid-base titrations in presence of
453 0.22 M Ca^{2+} (at I = 0.7 M) led to physically unreasonable curves, and a gelatinous
454 precipitate was observed at the end of the experiments. On the other hand, duplicate
455 titrations carried out in 0.01 M Ca^{2+} or Mg^{+2} (at I = 0.1 M) yielded no apparent
456 precipitate and almost identical results as in the absence of calcium/magnesium at the
457 same ionic strength. The titration curves were compared with NICA-Donnan
458 predictions using the fitted parameters from Table 1 and the generic values for the
459 intrinsic binding parameters of Ca^{2+} and Mg^{+2} (Milne et al., 2003), since the
460 experimental information is not enough to perform an optimization of the latter
461 parameters. The results (see Supplementary Material) are consistent with negligible
462 calcium/magnesium binding and, consequently, almost no competition between
463 protons and calcium or magnesium ions under these conditions.

464 **5.5 Relevance to modelling of trace metal binding by marine DOM**

465 The NICA-Donnan model assumes that trace metal ions compete to a greater or lesser
466 degree with protons and major ions for the binding to macromolecular sites. The
467 extent of this is the result of a complex interplay among the concentration of
468 competing ions, their intrinsic affinity parameters, ionic strength and inorganic
469 speciation of the metal ions, *e.g.* hydrolysis (Rey-Castro et al., 2009). To illustrate
470 this, we take the example of Fe(III), a bioessential micronutrient. We compare the
471 NICA-Donnan predictions of the amount of iron bound by marine DOM (Q_{Fe}) as a
472 function of salinity and pH using two different sets of parameters (see Figure 4).
473 These sets differ exclusively on the proton binding parameters, while the values for
474 Fe(III) are the same in both cases and taken from a previous work (Avendaño et al.,
475 2016). The contour plot in panel (a) was calculated with the marine DOM values
476 fitted in this work (parameter set a); whereas panel (b) used the corresponding generic
477 values for fulvic acid (parameter set b) (Milne et al., 2001). Further details are given
478 in the Supplementary Material.

479 As can be observed, the parameter set (a) leads to values of Q_{Fe} that are *ca*. one order
480 of magnitude lower than parameter set (b) at the same environmental conditions.
481 The conditional affinity spectra for Fe(III) in the calculated scenarios (see
482 Supplementary Material) show that the competitive effect of protons (and, to a much
483 lesser extent, Ca and Mg) induces a shift in the effective affinity of phenolic sites for
484 iron which results in an overlap with the carboxylic mode (which remains mostly
485 unoccupied, as shown in Figure 2b). This means that both kinds of sites participate in
486 the binding of iron ions. Consequently, the differences observed in the amount of iron
487 bound (Figure 4) are due to:

1) The decreased degree of heterogeneity of the first mode of binding sites in the extracted marine DOM. There is therefore a smaller fraction of carboxylic sites in the marine DOM with a high affinity for Fe(III) ions.

2) The variation in the maximum binding capacities: $Q_{\max H,1} + Q_{\max H,2}$ of marine DOM is ca. 60% lower than in the generic FA.

3) The differences in the Boltzmann factor for both marine DOM and generic FA. The values of V_D are somewhat larger for DOM than generic FA at the same salinity. The ion concentrations in the Donnan phase are therefore lower at the same ionic strength and macromolecular charge and, thus the variation of Q_{Fe} with salinity is less pronounced for marine DOM (Figure 4, panel (a)).

Finally, the relative gradient of Q_{Fe} with pH at constant salinity is similar for both marine DOM and generic FA, as it is mainly controlled by the dependence of iron hydroxide solubility with pH, while the H/Fe(III) exchange ratios are quite similar in both datasets. A more extensive discussion is included in the Supplementary Material. We must acknowledge the limitations in the predictive capacity of these scenarios, since the values of the iron binding parameters have not been optimized for this specific DOM fraction. Still, the differences between both scenarios reflect the potential implications of the variation in electrostatic and chemical proton binding parameters with the composition of DOM. In this way, the results of this work represent a useful first step in the development of a systematic model for the prediction of the ion binding characteristics of marine DOM. In addition to optimisation of extraction procedures and improvement in consistency in titration data obtained at pH> 9.5, future work should also address the correlation of the model parameters with spatial and seasonal variability of extracted DOM to achieve a representative description.

513 **5.6 Broader environmental implications**

514 Climate change effects will produce variations in pH, temperature, and oxygen
515 concentrations, with associated effects, in seawaters. Alterations in the chemical
516 composition of marine DOM due to global shifts in the future ocean are expected.
517 This broad pool of organic molecules contribute to the storage of atmospheric CO_2 in
518 the ocean, support ecosystems and influence (micronutrient) trace metal cycles, which
519 are essential for marine primary production, but can also produce toxic effects. For
520 example, these organic ligands are thought to increase iron solubility and thus the
521 overall iron inventory in the ocean, since via competition with hydroxide ions, they
522 counteract the tendency for precipitation of iron hydroxides (Liu and Millero, 2002).
523 Marine DOM-metal interactions are key to our understanding of trace metal binding
524 behaviour in seawater and should therefore be considered in global biogeochemical
525 models to evaluate future climate change scenarios, such as ocean acidification
526 (Avendaño et al., 2016; Gledhill et al., 2015; Ye et al., 2020). All these complex
527 interactions depend on the physicochemical properties of the groups that form the
528 marine DOM. Determination of the acid-base properties of DOM, which we
529 investigate here, can provide an accurate and quantitative description of these
530 chemical groups.

531

532 **6. Conclusions**

533 The NICA-Donnan model was able to fully describe the most acidic mode (carboxylic
534 groups) of marine DOM. This mode has a larger mean affinity for protons and a lower
535 heterogeneity degree than a generic fulvic acid but still within the reported variability
536 for fulvic acids of freshwater and terrestrial origin. Our DOM binding parameters are
537 similar to the few values found in literature for DOM extracted from estuarine,

coastal, and open ocean waters. No apparent effect of temperature (between 5 and 25ºC) or major seawater cations (Ca/Mg at representative concentrations) was noticed in the proton binding curves of marine DOM. The binding parameters derived from acid-base titrations are relevant for the prediction of binding of a trace metal such as iron to marine DOM.

Author contributions

Pablo Lodeiro: Conceptualization, Methodology, Investigation, Writing - Original Draft, Writing - Review & Editing, Supervision. **Carlos Rey-Castro:** Conceptualization, Methodology, Writing - Original Draft, Writing - Review & Editing. **Calin David:** Methodology, Software, Validation, Formal analysis, Data Curation, Visualization. **Eric P. Achterberg:** Resources, Writing - Review & Editing. **Jaume Puy:** Resources, Writing - Review & Editing. **Martha Gledhill:** Conceptualization, Writing - Review & Editing, Supervision, Project administration, Funding acquisition.

Data statement

The datasets generated during and/or analysed during the current study are available from the corresponding author on reasonable request.

Acknowledgements

The authors gratefully acknowledge support from the Deutsche Forschungsgemeinschaft (Project GL 807/2), the Spanish Ministerio de Economía y Competitividad (Project CTM2016-78798-C2-1-P) and the German Helmholtz

562 Association. The authors would also like to thank Dr. J.L. Garcés for his advice on the
563 calculation of the affinity spectra.
564

565 **References**

566 Avendaño L, Gledhill M, Achterberg EP, Rérolle VMC, Schlosser C. Influence of
567 Ocean Acidification on the Organic Complexation of Iron and Copper in
568 Northwest European Shelf Seas; a Combined Observational and Model Study.
569 Front. Mar. Sci. 2016; 3: 58. https://doi.org/10.3389/fmars.2016.00058
570 Benedetti MF, Van Riemsdijk WH, Koopal LK, Kinniburgh DG, Gooddy DC, Milne
571 CJ. Metal ion binding by natural organic matter: From the model to the field.
572 Geochim. Cosmochim. Acta 1996a; 60: 2503-2513.
573 https://doi.org/10.1016/0016-7037(96)00113-5
574 Benedetti MF, vanRiemsdik WH, Koopal LK. Humic substances considered as a
575 heterogeneous donnan gel phase. Environ. Sci. Technol. 1996b; 30: 1805-
576 1813. https://doi.org/10.1021/Es950012y
577 Brandariz I, Barriada JL, Vilarinio T, Sastre de Vicente ME. Comparison of several
578 calibration procedures for glass electrodes in proton concentration. Monatsh.
579 Chem. 2004; 135: 1475-1488. https://doi.org/10.1007/s00706-004-0239-x
580 Cai W-J, Wang Y, Hodson RE. Acid-Base Properties of Dissolved Organic Matter in
581 the Estuarine Waters of Georgia, USA. Geochim. Cosmochim. Acta 1998; 62:
582 473-483. https://doi.org/10.1016/S0016-7037(97)00363-3
583 Carlson CA, Hansell DA. Chapter 3 - DOM Sources, Sinks, Reactivity, and Budgets.
584 In: Hansell DA, Carlson CA, editors. Biogeochemistry of Marine Dissolved
585 Organic Matter (Second Edition). Academic Press, Boston, 2015, pp. 65-126.

586 Carvalhais N, Forkel M, Khomik M, Bellarby J, Jung M, Migliavacca M, et al. Global
587 covariation of carbon turnover times with climate in terrestrial ecosystems.
588 Nature 2014; 514: 213-217. https://doi.org/10.1038/nature13731
589 Christl I, Kretzschmar R. Relating Ion Binding by Fulvic and Humic Acids to
590 Chemical Composition and Molecular Size. 1. Proton Binding. Environ. Sci.
591 Technol. 2001; 35: 2505-2511. https://doi.org/10.1021/es0002518
592 David C, Mongin S, Rey-Castro C, Galceran J, Companys E, Garcés JL, et al.
593 Competition effects in cation binding to humic acid: Conditional affinity
594 spectra for fixed total metal concentration conditions. Geochim. Cosmochim.
595 Acta 2010; 74: 5216-5227. https://doi.org/10.1016/j.gca.2010.06.023
596 Deutsch B, Alling V, Humborg C, Korth F, Mörth CM. Tracing inputs of terrestrial
597 high molecular weight dissolved organic matter within the Baltic Sea
598 ecosystem. Biogeosciences 2012; 9: 4465-4475. https://doi.org/10.5194/bg-9-
599 4465-2012
600 Dittmar T, Koch B, Hertkorn N, Kattner G. A simple and efficient method for the
601 solid-phase extraction of dissolved organic matter (SPE-DOM) from seawater.
602 Limnol. Oceanogr-Meth. 2008; 6: 230-235.
603 https://doi.org/10.4319/lom.2008.6.230
604 Dittmar T, Stubbins A. 12.6 - Dissolved Organic Matter in Aquatic Systems. In:
605 Holland HD, Turekian KK, editors. Treatise on Geochemistry (Second
606 Edition). Elsevier, Oxford, 2014, pp. 125-156.
607 Gledhill M, Achterberg EP, Li K, Mohamed KN, Rijkenberg MJA. Influence of ocean
608 acidification on the complexation of iron and copper by organic ligands in
609 estuarine waters. Mar. Chem. 2015; 177: 421-433.
610 https://doi.org/10.1016/j.marchem.2015.03.016

611 Gledhill M, Buck KN. The organic complexation of iron in the marine environment: a
612 review. Front. Microbiol. 2012; 3: 69.
613 https://doi.org/10.3389/fmicb.2012.00069
614 Gledhill M, van den Berg CMG. Determination of complexation of iron(III) with
615 natural organic complexing ligands in seawater using cathodic stripping
616 voltammetry. Mar. Chem. 1994; 47: 41-54. https://doi.org/10.1016/0304-
617 4203(94)90012-4
618 Green NW, Perdue EM, Aiken GR, Butler KD, Chen H, Dittmar T, et al. An
619 intercomparison of three methods for the large-scale isolation of oceanic
620 dissolved organic matter. Mar. Chem. 2014; 161: 14-19.
621 https://doi.org/10.1016/j.marchem.2014.01.012
622 Hansell DA. Recalcitrant Dissolved Organic Carbon Fractions. Annu. Rev. Mater.
623 Sci. 2013; 5: 421-445. https://doi.org/10.1146/annurev-marine-120710-100757
624 Hawkes JA, Sjöberg PJR, Bergquist J, Tranvik LJ. Complexity of dissolved organic
625 matter in the molecular size dimension: insights from coupled size exclusion
626 chromatography electrospray ionisation mass spectrometry. Faraday Discuss.
627 2019; 218: 52-71. https://doi.org/10.1039/C8FD00222C
628 Hertkorn N, Benner R, Frommberger M, Schmitt-Kopplin P, Witt M, Kaiser K, et al.
629 Characterization of a major refractory component of marine dissolved organic
630 matter. Geochim. Cosmochim. Acta 2006; 70: 2990-3010.
631 https://doi.org/10.1016/j.gca.2006.03.021
632 Hoikkala L, Kortelainen P, Soinne H, Kuosa H. Dissolved organic matter in the Baltic
633 Sea. J. Marine Syst. 2015; 142: 47-61.
634 https://doi.org/10.1016/j.jmarsys.2014.10.005

635 Huizenga DL, Kester DR. Protonation equilibria of marine dissolved organic matter1.
636 Limnology and Oceanography 1979; 24: 145-150.
637 https://doi.org/10.4319/lo.1979.24.1.0145
638 Kinniburgh DG, Milne CJ, Benedetti MF, Pinheiro JP, Filius J, Koopal LK, et al.
639 Metal Ion Binding by Humic Acid: Application of the NICA-Donnan Model.
640 Environ. Sci. Technol. 1996; 30: 1687-1698.
641 https://doi.org/10.1021/es950695h
642 Kinniburgh DG, van Riemsdijk WH, Koopal LK, Borkovec M, Benedetti MF, Avena
643 MJ. Ion binding to natural organic matter: competition, heterogeneity,
644 stoichiometry and thermodynamic consistency. Colloid Surf. A-Physicochem.
645 Eng. Asp. 1999; 151: 147-166. https://doi.org/10.1016/S0927-7757(98)00637-
646 2
647 Koopal LK, Saito T, Pinheiro JP, Riemsdijk WHv. Ion binding to natural organic
648 matter: General considerations and the NICA–Donnan model. Colloid Surf. A-
649 Physicochem. Eng. Asp. 2005; 265: 40-54.
650 https://doi.org/10.1016/j.colsurfa.2004.11.050
651 Koopal LK, Vanriemsdijk WH, Dewit JCM, Benedetti MF. Analytical Isotherm
652 Equations for Multicomponent Adsorption to Heterogeneous Surfaces. J.
653 Colloid Interface Sci. 1994; 166: 51-60. https://doi.org/10.1006/jcis.1994.1270
654 Kuliński K, Schneider B, Hammer K, Machulik U, Schulz-Bull D. The influence of
655 dissolved organic matter on the acid–base system of the Baltic Sea. J. Marine
656 Syst. 2014; 132: 106-115. https://doi.org/10.1016/j.jmarsys.2014.01.011
657 Li Y, Harir M, Lucio M, Kanawati B, Smirnov K, Flerus R, et al. Proposed
658 Guidelines for Solid Phase Extraction of Suwannee River Dissolved Organic

659 Matter. Anal. Chem. 2016; 88: 6680-6688.
660 https://doi.org/10.1021/acs.analchem.5b04501
661 Li Y, Harir M, Uhl J, Kanawati B, Lucio M, Smirnov KS, et al. How representative
662 are dissolved organic matter (DOM) extracts? A comprehensive study of
663 sorbent selectivity for DOM isolation. Water Res. 2017; 116: 316-323.
664 https://doi.org/10.1016/j.watres.2017.03.038
665 Liu X, Millero FJ. The solubility of iron in seawater. Mar. Chem. 2002; 77: 43-54.
666 https://doi.org/10.1016/S0304-4203(01)00074-3
667 Lodeiro P, Martínez-Cabanas M, Herrero R, Barriada JL, Vilariño T, Rodríguez-
668 Barro P, et al. The proton binding properties of biosorbents. Environ. Chem.
669 Lett. 2019; 17: 1281–1298. https://doi.org/10.1007/s10311-019-00883-z
670 Martín Hernández-Ayon J, Zirino A, Dickson AG, Camiro-Vargas T, Valenzuela-
671 Espinoza E. Estimating the contribution of organic bases from microalgae to
672 the titration alkalinity in coastal seawaters. Limnol. Oceanogr-Meth. 2007; 5:
673 225-232. https://doi.org/10.4319/lom.2007.5.225
674 MATLAB. Release 2019b. The MathWorks, Inc., Natick, Massachusetts, United
675 States, 2019. Doi.
676 Milne CJ, Kinniburgh DG, Tipping E. Generic NICA-Donnan model parameters for
677 proton binding by humic substances. Environ. Sci. Technol. 2001; 35: 2049-
678 2059. https://doi.org/10.1021/es000123j
679 Milne CJ, Kinniburgh DG, van Riemsdijk WH, Tipping E. Generic NICA−Donnan
680 Model Parameters for Metal-Ion Binding by Humic Substances. Environ. Sci.
681 Technol. 2003; 37: 958-971. https://doi.org/10.1021/es0258879
682 Ohshima H. Theory of colloid and interfacial electric phenomena. Amsterdam ;
683 Boston: Elsevier Academic Press, 2006.

684 Ohshima H. Donnan potential and surface potential of a spherical soft particle in an
685 electrolyte solution. J. Colloid Interface Sci. 2008; 323: 92-97.
686 https://doi.org/10.1016/j.jcis.2008.03.021
687 Pernet-Coudrier B, Companys E, Galceran J, Morey M, Mouchel J-M, Puy J, et al.
688 Pb-binding to various dissolved organic matter in urban aquatic systems: Key
689 role of the most hydrophilic fraction. Geochim. Cosmochim. Acta 2011; 75:
690 4005-4019. https://doi.org/10.1016/j.gca.2011.04.030
691 Powers LC, Hertkorn N, McDonald N, Schmitt-Kopplin P, Del Vecchio R, Blough
692 NV, et al. Sargassum sp. Act as a Large Regional Source of Marine Dissolved
693 Organic Carbon and Polyphenols. Global Biogeochem. Cycles 2019; 33:
694 1423-1439. https://doi.org/10.1029/2019GB006225
695 Repeta DJ. Chapter 2 - Chemical Characterization and Cycling of Dissolved Organic
696 Matter. In: Hansell DA, Carlson CA, editors. Biogeochemistry of Marine
697 Dissolved Organic Matter (Second Edition). Academic Press, Boston, 2015,
698 pp. 21-63.
699 Rey-Castro C, Mongin S, Huidobro C, David C, Salvador J, Garcés JL, et al.
700 Effective Affinity Distribution for the Binding of Metal Ions to a Generic
701 Fulvic Acid in Natural Waters. Environ. Sci. Technol. 2009; 43: 7184-7191.
702 https://doi.org/10.1021/es803006p
703 Seidel M, Manecki M, Herlemann DPR, Deutsch B, Schulz-Bull D, Jürgens K, et al.
704 Composition and Transformation of Dissolved Organic Matter in the Baltic
705 Sea. Front. Earth Sci. 2017; 5: 31. https://doi.org/10.3389/feart.2017.00031
706 Tipping E. Cation Binding by Humic Substances. Cambridge: Cambridge University
707 Press, 2002.

708 Turner DR, Achterberg EP, Chen C-TA, Clegg SL, Hatje V, Maldonado MT, et al.
709 Toward a Quality-Controlled and Accessible Pitzer Model for Seawater and
710 Related Systems. Front. Mar. Sci. 2016; 3: 139.
711 https://doi.org/10.3389/fmars.2016.00139
712 Ulfsbo A, Kuliński K, Anderson LG, Turner DR. Modelling organic alkalinity in the
713 Baltic Sea using a Humic-Pitzer approach. Mar. Chem. 2015; 168: 18-26.
714 https://doi.org/10.1016/j.marchem.2014.10.013
715 Xu J, Koopal LK, Fang L, Xiong J, Tan W. Proton and Copper Binding to Humic
716 Acids Analyzed by XAFS Spectroscopy and Isothermal Titration Calorimetry.
717 Environ. Sci. Technol. 2018; 52: 4099-4107.
718 https://doi.org/10.1021/acs.est.7b06281
719 Yang B, Byrne RH, Lindemuth M. Contributions of organic alkalinity to total
720 alkalinity in coastal waters: A spectrophotometric approach. Mar. Chem.
721 2015; 176: 199-207. https://doi.org/10.1016/j.marchem.2015.09.008
722 Ye Y, Völker C, Gledhill M. Exploring the iron-binding capacity of the ocean using a
723 combined pH and DOC parameterisation. Global Biogeochem. Cycles 2020;
724 In press.
725 Zark M, Dittmar T. Universal molecular structures in natural dissolved organic
726 matter. Nat. Commun. 2018; 9: 3178. https://doi.org/10.1038/s41467-018-
727 05665-9
728

Table 1: Optimized NICA-Donnan parameter values (V_D: volume of the gel phase; $Q_{maxH,j}$: total amount of available proton binding sites within each distribution; $\log \bar{k}_{H,j}$: median value of the j^{th} affinity distribution for protons; m_j: width of the affinity distribution function; RMSE: root-mean square error) for proton binding at 25ºC.

Donnan sub-model	V_D parameter	$Q_{max\,H,1}$ (mol·kg^{-1})	$\log \bar{k}_{H,1}$	m_1	$Q_{max\,H,2}$ (mol·kg^{-1})	$\log \bar{k}_{H,2}$	m_2	RMSE (mol·kg^{-1})
Standard eq. **S12**	b = 0.70	2.52	3.26	0.69	**0.80** [a]	**8.60** [b]	**0.53** [b]	0.060
PB-V_D eq. **S13**	a = 0.036	2.55	3.82	0.59	**0.81** [a]	**9.41** [c]	**0.49** [c]	0.069
'*ad hoc*'	reference: I = 0.7 M	2.52	3.79	0.55	**0.80** [a]	**9.41** [c]	**0.49** [c]	0.072

The values in bold were constrained as follows: [a] The ratio $Q_{max\,H,2}/Q_{max\,H,1}$ was kept fixed at 0.32 as in the generic parameterization for fulvic acid (Milne et al. 2001). [b] Generic values for fulvic acid (Milne et al. 2001). [c] estimated at I = 0.7 M using the generic intrinsic NICA parameters for fulvic acid. The comparison between NICA-Donnan model and experimental values is shown in Figure 1.

Table 2: DOM sizes estimated from V_D at different ionic strengths.

I (mol·L^{-1})	κ^{-1} (nm)[a]	V_D (L·kg^{-1})[b]	$\kappa \cdot r$ [c]	$\kappa \cdot d_{av}$ [d]
0.01	3.6	16-71	0.4-0.7	0.7-1.1
0.02	2.3	9-49	0.5-0.9	0.9-1.6
0.1	1.0	2.6-17	0.9-1.6	1.5-2.7
0.7	0.4	0.7-n.a.[e]	1.7-n.a. [e]	2.8-n.a. [e]

[a] Debye length at 298K. [b] Range of fitted V_D values, where lower and upper bounds corresponds to standard and '*ad hoc*' Donnan models, respectively (see Figure 3). [c] Values calculated with eq. S15 using ρ = 1.4-2.0 kg/L (Benedetti et al. 1996) and a reference M_w value of 500 Da. [d] Average distance (in Debye length units) between charged groups calculated as $d_{av} = 2r/Z_{\max}^{1/3}$ using an average amount of charged groups per molecule $Z_{\max} = M_w \times \left(Q_{\max H,1} + Q_{\max H,2}\right)$ of 1.7 (reference M_w = 500 Da). [e] The '*ad hoc*' model assumes negligible electrostatic contribution at I = 0.7 M.

References

Benedetti MF, vanRiemsdik WH, Koopal LK (1996) Humic substances considered as a heterogeneous donnan gel phase. Environmental Science & Technology 30: 1805-1813. Doi: 10.1021/Es950012y

Milne CJ, Kinniburgh DG, Tipping E (2001) Generic NICA-Donnan model parameters for proton binding by humic substances. Environmental Science & Technology 35: 2049-2059. Doi: 10.1021/es000123j

Figures
Click here to download Figure: Figures.doc

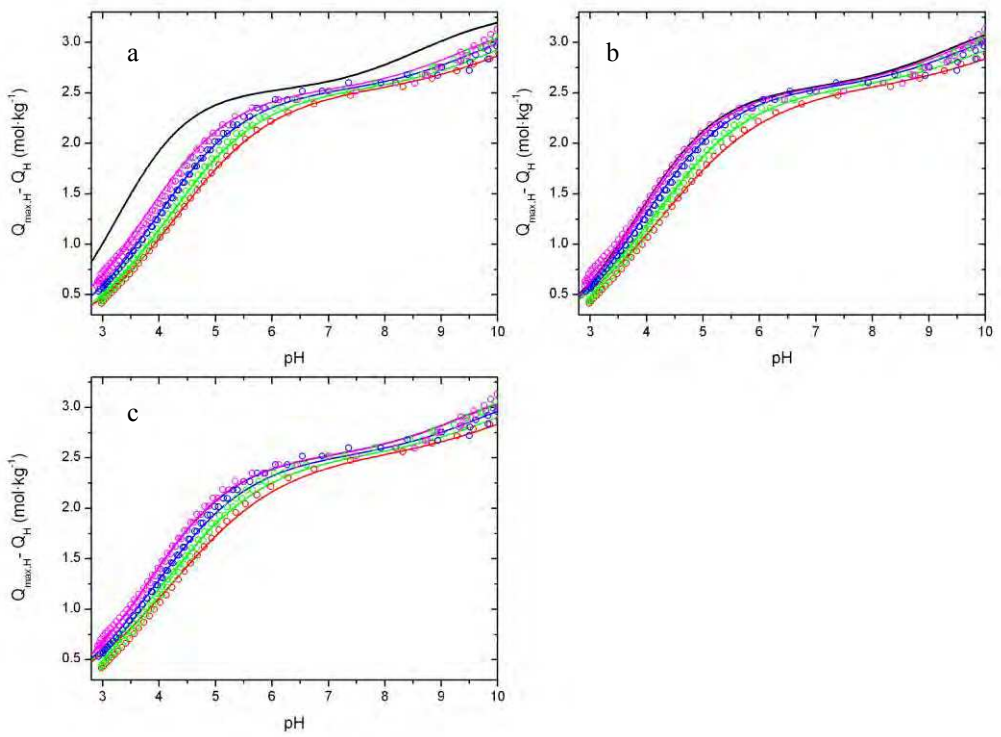

Figure 1: NICA-Donnan fits to proton titration data of marine DOM at 25ºC using V_D models: (a) standard, eq. S12; (b) PB-V_D, eq. S13; (c) '*ad hoc*' with reference curve at I=0.7 M. Symbols: experimental values; lines: model fits. The ionic strength values are (from bottom to top): 0.01 (red), 0.02 (green), 0.1 (blue) and 0.7 (pink) M. The uppermost black curve corresponds to the 'master curve' charge *vs*. pH_D (in panels b and c it lies below the experimental curve at I = 0.7 M).

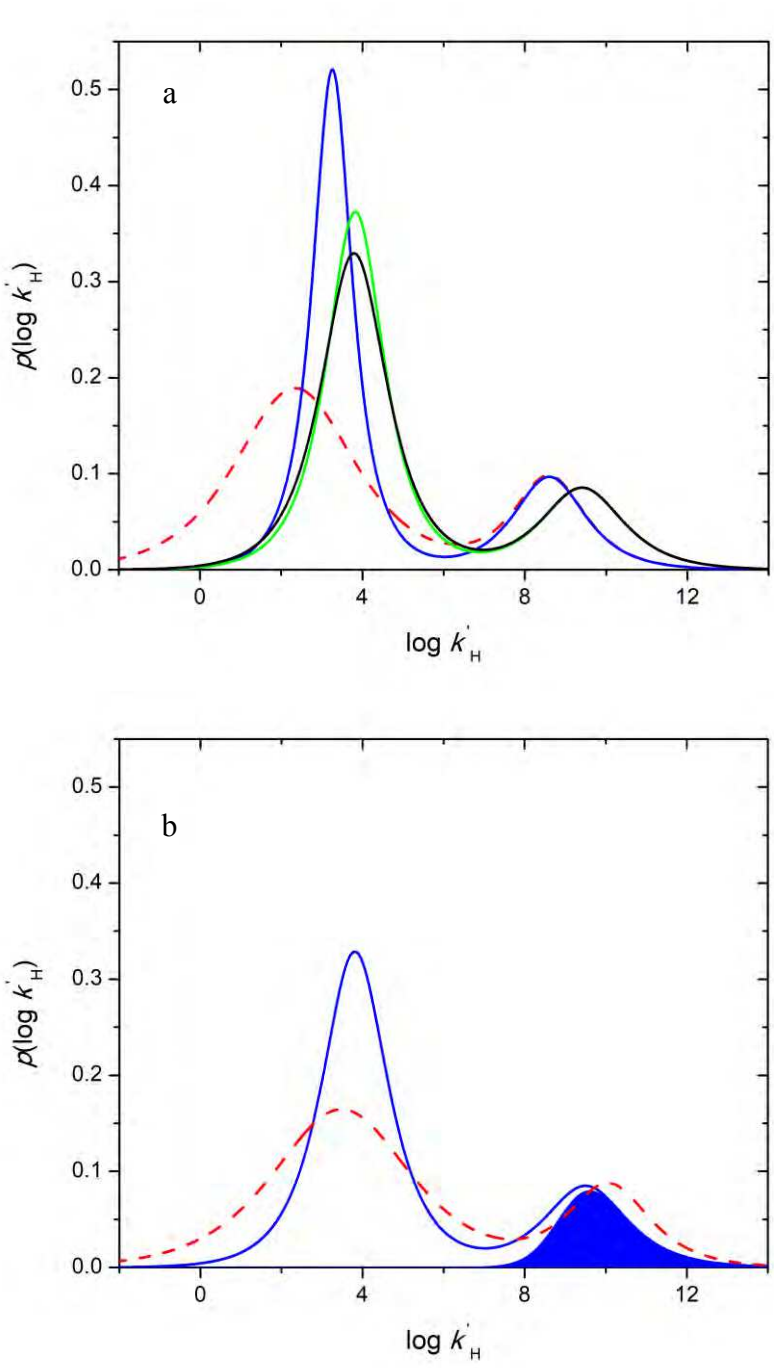

Figure 2: (a) Intrinsic proton affinity spectra of marine DOM calculated from the NICA parameters of Table 1 using: standard V_D (blue), PB- V_D (green) and '*ad hoc*' (black) Donnan models. **(b)** Effective proton affinity spectrum of marine DOM at I = 0.32 M (solid blue line) and density of protonated DOM sites at pH 8.36 (shaded blue area), calculated with NICA and standard V_D parameters from Table 1 (the three Donnan models lead to virtually identical effective spectra). The intrinsic and effective (I = 0.32 M) spectra of a generic fulvic acid (Milne et al. 2001) are included as red dashed lines in panels (a) and (b), respectively, for comparison purposes. All spectra are normalized.

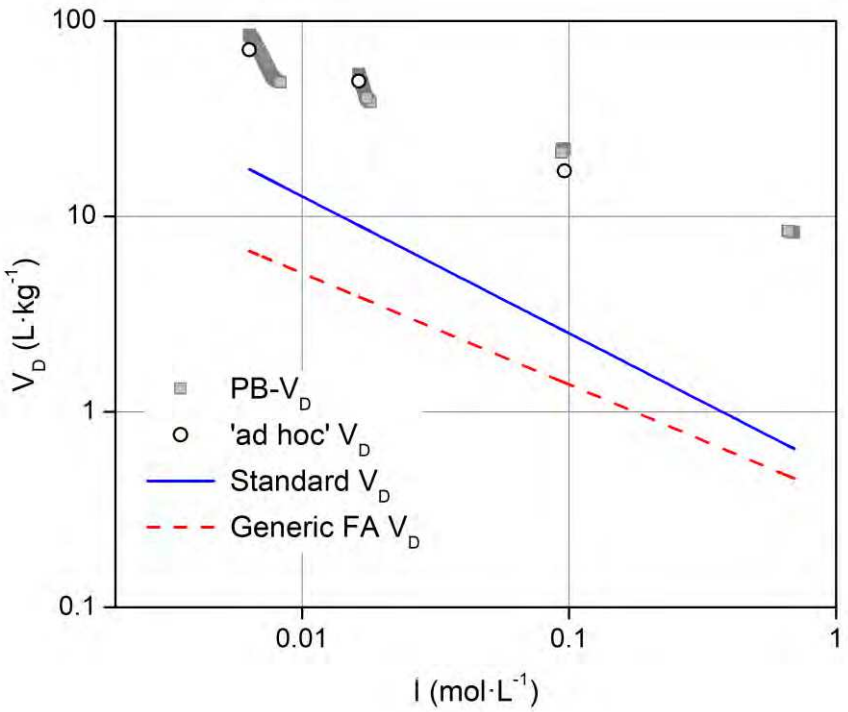

Figure 3: Values of V_D obtained from fits to proton titration data of marine DOM at 25ºC using different Donnan models: PB-V_D (squares), '*ad hoc*' (open circles), standard model using fitted *b* parameter (blue line), and standard model using the generic value of *b* for fulvic acids (red dashed line).

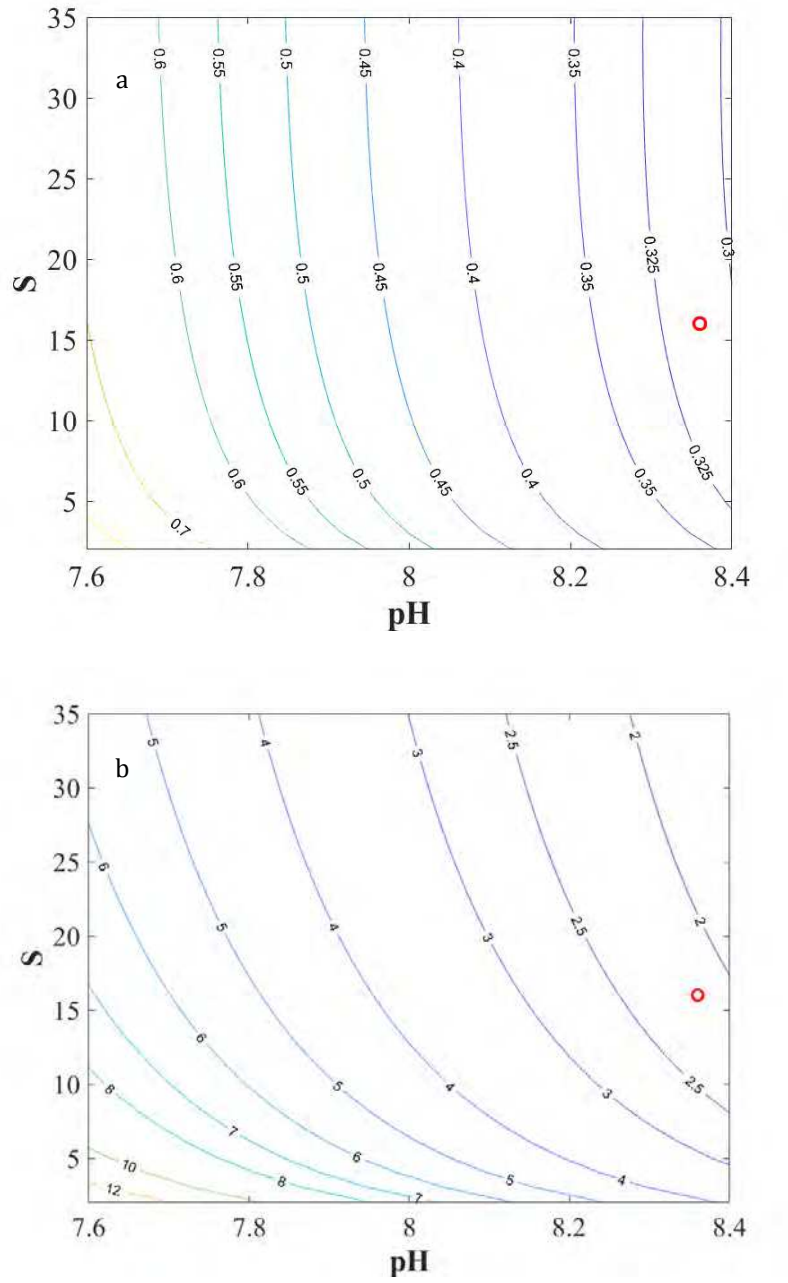

Figure 4: Contour plots of the estimated Fe(III) binding to marine DOM, Q_{Fe} (mmol·kg^{-1}), as a function of salinity (S) and pH within the typical values of surface waters of Baltic Sea (the red circle represents actual conditions at the sampling site), calculated by NICA-Donnan model assuming that free Fe^{3+} ion concentration is controlled by the solubility equilibrium of $Fe(OH)_{3(s)}$ at 15ºC. Dataset (a): values of $Q_{\max H,1}$, $Q_{\max H,2}$, $\overline{k}_{H,1}$, m_1 and b reported in this work; dataset (b): generic values of $Q_{\max H,1}$, $Q_{\max H,2}$, $\overline{k}_{H,1}$, m_1 and b for fulvic acid (Milne et al. 2001). The binding parameters of Fe(III) are identical in both cases. See Supplementary Material for further details.

References

Milne CJ, Kinniburgh DG, Tipping E (2001) Generic NICA-Donnan model parameters for proton binding by humic substances. Environmental Science & Technology 35: 2049-2059. Doi: 10.1021/es000123j

Supplementary material for on-line publication only

Click here to download Supplementary material for on-line publication only: Supplementary_Material.pdf